

1 **Why does the metabolic cost of walking increase on compliant substrates?**

2

3 Barbara Grant^{1*}, James Charles¹, Brendan Geraghty¹, James Gardiner¹, Kristiaan D’Août¹, Peter L.
4 Falkingham² & Karl T. Bates¹.

5

6 ¹Department of Musculoskeletal & Ageing Science, Institute of Life Course & Medical Sciences,
7 University of Liverpool, The William Henry Duncan Building, 6 West Derby Street, Liverpool L7
8 8TX, UK;

9 ²School of Biological and Environmental Sciences, Liverpool John Moores University, James
10 Parsons Building, Bryon Street, Liverpool L3 3AF, UK

11

12

13 *Correspondence to: barbara.grant@liverpool.ac.uk

14 **Key words:** biomechanics, locomotion, energetics, musculoskeletal model, compliant substrate

15

16 SUMMARY

17 Walking on compliant substrates requires more energy than walking on hard substrates but the
18 biomechanical factors that contribute to this increase are debated. Previous studies suggest various
19 causative mechanical factors, including disruption to pendular energy recovery, increased muscle
20 work, decreased muscle efficiency and increased gait variability. We test each of these hypotheses
21 simultaneously by collecting a large kinematic and kinetic data set of human walking on foams of
22 differing thickness. This allowed us to systematically characterise changes in gait with substrate
23 compliance, and, by combining data with mechanical substrate testing, drive the very first subject-
24 specific computer simulations of human locomotion on compliant substrates to estimate the internal
25 kinetic demands on the musculoskeletal system. Negative changes to pendular energy exchange or
26 ankle mechanics are not supported by our analyses. Instead we find that the mechanistic causes of
27 increased energetic costs on compliant substrates are more complex than captured by any single
28 previous hypothesis. We present a model in which elevated activity and mechanical work by
29 muscles crossing the hip and knee are required to support the changes in joint (greater excursion
30 and maximum flexion) and spatiotemporal kinematics (longer stride lengths, stride times and stance
31 times, and duty factors) on compliant substrates.

32 **1. Introduction**

33 The evolution of animal locomotion has mostly occurred on substrates with complex heterogeneous
34 topography and material properties. However, our current understanding of animal gait and
35 energetics is dominated by studies on hard, level surfaces in laboratories, which do not reflect most
36 naturally occurring terrains. Recent work on humans has shown that locomotion on complex
37 substrates like loose rock surfaces [1], ballast [2], uneven [3, 4] and compliant [5-10] terrains is
38 typically associated with an increase in energy expenditure relative to uniform, non-deforming
39 substrates. Indeed, variations in the compliance or stiffness of footwear has also been shown to
40 systematically affect locomotor costs [11, 12]. The term ‘compliant’ has been used broadly within
41 the field [4-9] to refer to any substrate that has non-negligible deformation under loads typically
42 generated during human locomotion. A substantial body of literature has sought to understand
43 elevated energetic costs on compliant substrates like sand, mud and snow [5-7, 13] but at present
44 there remains little consensus about the primary mechanistic causes.

45

46 Lejeune et al. [7] and Zamparo et al. [6] compared the change in the energetic cost of transport
47 (CoT) on sand across a range of speeds. These studies discovered different magnitudes and nature
48 of change in CoT with speed on compliant sands and invoked different biomechanical mechanisms
49 to explain these increases. Lejeune et al. [7] attributed the higher energetic costs to an increase in
50 muscle-tendon work and a decrease in muscle-tendon efficiency whereas Zamparo et al. [6]
51 proposed that it was due to a lower energy recovery through a reduction in the efficiency of
52 pendular energy exchange in walking and in the reduced recovery of elastic energy storage in
53 running.

54

55 Pinnington and Dawson [8] suggested a potential increase in muscle co-activation and an increase
56 in foot contact time on compliant substrates may lead to increased oxygen consumption due to a
57 reduction in elastic energy storage and recovery, and ultimately a decrease in muscle-tendon
58 efficiency. These authors noted that foot slippage may also play a role, as postulated by Zamparo et
59 al. [6]. Voloshina et al. [3] found an increase in mean muscle activity and increased mechanical
60 work on uneven substrates and suggested there may be a potential increase in muscle co-activation.
61 Bates et al. [14] speculated that increased activation of ankle extensors, specifically, may be a major
62 contributor to increased CoT on sand. Pandolf et al. [13] proposed that increasing work to lift the
63 Centre of Mass (CoM), a stooping posture and difficulties maintaining stability are the primary
64 causes of increased CoT when walking on snow.

65

66 Therefore, while it is widely accepted that compliant substrates incur an increase in CoT, there
67 remains considerable uncertainty about the relative contribution of different biomechanical factors
68 underpinning this increase. Possible reasons include the measurement of different variables across
69 studies [10], variation in footwear (e.g. barefoot, different types of shoes; but see [8]), substrates
70 used, and the gaits and speeds tested. Unfortunately, the absence of quantification of the mechanical
71 properties of the compliant substrates used across past studies impedes comparison. In this study,
72 we attempt to address these issues and provide an exhaustive evaluation of why the energetic cost
73 of walking increases as substrate compliance increases. To achieve this, we present a large
74 experimental kinematic and kinetic data set of human walking on foams of differing thickness, with
75 detailed characterisation of substrate mechanical properties by uniaxial compression testing.
76 Quantification of substrate properties not only facilitates repeatability and systematic comparison to
77 other substrates but also allows us to us to carry out subject-specific computer simulations of
78 locomotion across compliant substrates. This validated individualised computational framework
79 [15] allows for the prediction of aspects of internal kinetics and muscle performance that cannot be
80 measured non-invasively, and thus may provide further insights into the mechanisms behind

81 locomotor cost beyond those allowed by experimental methods alone. Through this integrated
82 experimental-computational workflow we test the previously proposed hypotheses that increased
83 CoT on compliant substrates is primarily the result of (HYP1) negative disruption to pendular
84 energetic exchange [6], (HYP2a) increased muscle activation throughout the support limb [3] or
85 (HYP2b) within specific muscle groups [14], (HYP3) increased musculotendon unit (MTU) work
86 and decreased efficiency [7] and/or (HYP4) correcting greater instabilities indicated by increased
87 variability in gait [13].

88

89

90 **2. Material and Methods**

91 **(a) Experimental data collection**

92 30 young, healthy individuals (15 males, 15 females; age = 27.4 ± 3.8 years; height = 1.76 ± 0.1 m;
93 body mass = 71.1 ± 9.0 kg; body mass index = 23.0 ± 2.1 kgm⁻²; see Table S1; Exclusion Criteria
94 Text. S1) signed informed consent before participating in the study in accordance with ethical
95 approval from the University of Liverpool's Central University Research Ethics Committee for
96 Physical Interventions (#3757). Data were collected as part of a larger study [16]. As described in
97 this previous study, we used a K5 wearable metabolic unit (COSMED, Rome) to measure and
98 quantify the energy efficiency of walking of each subject on different types of terrain. Oxygen
99 uptake ($\text{VO}_2 \text{ mlO}_2\text{s}^{-1}$) and carbon dioxide produced ($\text{CO}_2 \text{ mlO}_2\text{s}^{-1}$) were measured continuously
100 during 7 minutes of barefoot walking in a breath-by-breath analysis on three surfaces: 1) hard, level
101 floor 2) a 13.2m long compliant polyether polyurethane foam with a thickness of 6 cm ("Thin
102 foam") and 3) the same foam of 13 cm thickness ("Thick foam") (eFoam.co.uk. Medium Foam.
103 Density Range: 31-34 kgm⁻³, Hardness strength: 100-130Nm; see Fig. S1). Subjects walked back
104 and forth across the walkways continuously at a self-selected speed during the 7 minute periods.
105 From these data, Charles et al. [16] previously found that walking cost of transport (CoT)

106 significantly increased with foam thickness ($p \leq 0.05$; Fig. S2), with CoT highest on the Thick foam
107 ($14.25 \pm 3.17 \text{ mlO}_2\text{m}^{-1}$), and lowest on the floor ($8.02 \pm 1.84 \text{ mlO}_2\text{m}^{-1}$) (Fig. S2).

108

109 Not discussed or analysed in this previous study [12], all participants also had 3D kinematics,
110 ground reaction forces and surface electromyography (EMG) measured synchronously during trials.

111 During the continuous walking on each substrate, the foams were placed over 3 in-series force
112 plates (Kistler 9281E) in the centre of their length, with 3D kinematics, ground reaction forces

113 (GRFs) and EMG recorded for 30 s at every minute from 3 min onwards. To increase sample size

114 and examine gait changes outside the context of longer, continuous bouts of walking, an additional

115 15 single trials were collected where a participant completed a single continuous passage across the

116 substrates (with substrate order randomised) while only 3D kinematics and EMG were measured.

117 For all trials, whole-body kinematics were recorded at 200Hz using 69 reflective markers and a 12-

118 camera Qualisys Oqus 7 motion capture system (Qualisys Inc., Göteborg, Sweden). Kinematic

119 data processing was undertaken in Visual3D (C-Motion Inc., Germantown, MD, USA) with a

120 kinematic model comprised of 13 segments: bilateral feet, shanks, thighs, upper arms, forearms, and

121 head, trunk and pelvis. From this data, Visual3D calculated CoM motions by using the position of

122 the kinematic model in relation to the lab based on mechanical principle patterns [17]. Gait events

123 were calculated automatically using a co-ordinate based algorithm [18] but checked manually for

124 every trial. Heel-strike was taken as the first weight-bearing contact between the substrate and the

125 foot and toe-off was taken as the last weight-bearing contact between the substrate and the hallux.

126

127 Marker tracking and EMG registration were all synchronized. EMGs were recorded using the

128 wireless Trigno EMG (Delsys, MA, USA) system at a sampling rate of 1110 Hz. Standard EMG

129 skin preparation methods were utilised [19] and the electrodes were positioned to record the activity

130 of 8 left lower extremity muscles: biceps femoris (BFL), rectus femoris (RF), vastus lateralis (VL),

131 vastus medialis (VM), tibialis anterior (TA), lateral gastrocnemius (LG), medial gastrocnemius

132 (MG) and soleus (SOL). Due to synchronization issues, EMG data for participants 1-6 were not
133 included. All EMG processing was performed in MATLAB v.2019b (Mathworks, Natick, USA).
134 The raw EMG signals were high pass filtered at 12Hz with a second-order Butterworth filter, full-
135 wave rectified and cropped to individual gait cycles. These data were then normalised (nEMG) to
136 maximum amplitude during all walking trials to allow for between-participant comparison, and the
137 integrated values were calculated (iEMG).

138
139 Mechanical energy data was processed in MATLAB and yielded gravitational potential energy
140 (E_{pot}), kinetic energy (E_{kin}) and total mechanical energy (E_{tot}) of the mass-normalised 3D CoM. The
141 recovery of mechanical energy (expressed as a percentage; R), relative amplitude (RA) and
142 congruity (the time when potential energy and kinetic energy are moving in the same direction; CO)
143 were calculated [20].

144

145 **(b) Statistical analysis of experimental data**

146

147 Joint kinematics were analysed using two statistical approaches: One dimensional statistical
148 parametric mapping (1D-SPM) [21], and Linear mixed-effect models (LMMs). 1D-SPM has the
149 benefit of allowing continuous statistical analysis without treating time points as independent, but
150 does not allow incorporation of additional factors (e.g. random or fixed effects) as LMMs do. 1D-
151 SPM analyses were performed using MATLAB to compare hip, knee and ankle joint angles across
152 substrates, with null hypothesis of no difference and alpha of 0.05. Joint angles at gait events (heel-
153 strike and toe-off), spatio-temporal data, iEMG data and mass-normalised mechanical energy
154 exchange variables were analysed using LMMs, where restricted maximum likelihood was used to
155 assess the significance of the fixed effects, substrate and trial type (continuous walking and single
156 trials) in explaining variation. As gait speed [22] and gender [23] can have an effect on gait
157 biomechanics, LMMs were repeated with the inclusion of speed and gender set as fixed effects.

158 Subjects were set as random effects, which allowed different intercepts for each subject. All
159 LMM's were performed in R [24] using the lmer function in the R package lme4 [25] and lmerTest
160 [26]. The coefficient of variation (CV) was calculated for all spatio-temporal data as a measure of
161 gait variability. Examples of the R and Matlab code used above are provided in the supplementary
162 material.

163

164 **(c) Material testing of substrates**

165 Mechanical behaviour of the thin and thick foam substrates was characterised by uniaxial
166 compression using an Instron 3366 universal testing machine (UTS) with a 2350 series 5kN load
167 cell (Instron, Norwood, MA) attached. A 203mm diameter flat indenter foot was connected to the
168 load cell by means of a swivel joint and the UTS was fitted with a bespoke horizontal base plate to
169 support the samples during testing. The base plate was perforated with 6.5mm diameter holes at
170 20mm centres to allow for rapid escape of air from the sample during the test [27]. Initial trials were
171 carried out to assess the effect of cyclic loading and strain rate on the samples. Ultimately, one
172 380mm x 380mm sample of each thickness was subjected to a single loading cycle at a rate of
173 500mm/min up to a compressive strain of 90%. The indenter load and displacement were recorded
174 and used to calculate the corresponding compressive strain, stress and modulus of the foam
175 substrates. Collectively, these data were used to provide gross quantification of the mechanical
176 behaviour of the foams for repeatability and comparability to other substrates, and to derive
177 simplified representations of material properties required for multi-body dynamics analysis (for
178 further detail, see Text S2- S3).

179

180

181 **(d) Multi-body dynamics (MDA) analysis**

182 To investigate potential internal kinetic mechanisms behind differences in CoT between the hard
183 floor and foam surfaces, one walking cycle was simulated over each substrate with one subject-

184 specific, 12 joint degree of freedom, 92 musculotendon unit (MTU) actuated lower limb
185 musculoskeletal model in OpenSim 4.2 [28] (Figure 1; age= 23, height= 180 cm, body mass= 77.4
186 kg; BMI= 23.8 kgm⁻²). This model is part of a previously published set of subject-specific models
187 [29] and freely available at the following link ([10.17638/datacat.liverpool.ac.uk/1536](https://datacat.liverpool.ac.uk/1536)). Note that in
188 the previous study and its data deposit [16], the model is referred to Subject 4. In this current study,
189 the participant is labelled as Subject 9 (Table S1). This model included muscle-force generating
190 properties from the subject's MRI that was matched to the subject's own kinematics collected in
191 this study. This subject was selected as their lower limb kinematics during walking on all substrates
192 fell entirely within one standard deviation of the means for all subjects throughout each gait cycle
193 (Fig S3). Inverse kinematics was used to generate the generalised coordinates of each unlocked
194 degree of freedom from the motion capture marker positions, and computed muscle control (CMC)
195 was used to predict muscle activations and powers during walking over each surface.
196 Experimentally measured GRFs recorded during the floor walking trials were applied to the model
197 to simulate walking on the hard floor. Contact geometries were used to simulate contact between
198 the foot and the foam surfaces during the thin and thick foam walking simulations. Here, contact
199 spheres were placed at the CoM of the calcaneus, forefoot and toes bodies of each lower limb to
200 represent the soft tissue of each foot segment, while a contact half-space was placed at different
201 heights to represent each foam surface (thin foam = 6cm; thick foam = 13cm). In OpenSim, the
202 contact forces between each sphere and the foam surfaces were defined as Hunt Crossley forces
203 [30], where the stiffness parameters were set at 0.047 MPa (47005 Nm⁻²) for the thin foam and
204 0.029 MPa (28763 Nm⁻²) for the thick foam. These stiffness values were derived from the uniaxial
205 behaviour of the foams using the Hertz contact equation for a cylindrical indenter and based on the
206 subjects body mass of 77.4kg. Since OpenSim is restricted to modelling linear behaviour and the
207 polyether polyurethane foam exhibits nonlinear behaviour, an average stiffness value was
208 determined for each foam based on the results of the compression testing. The other contact

209 parameters were set at the following values in each model: dissipation = 0.5 (ms^{-1}), static friction =
210 0.8, dynamic friction = 0.4, viscous friction = 0.4.

211

212 In each simulation, the activations of the BFL, RF, VL, VM, TA, LG, MG and SOL MTUs were
213 constrained to match the muscle activities measured experimentally using EMG as much as
214 possible. Residual and reserve actuators were applied to each unlocked degree of freedom in all
215 simulations to provide forces to the model if the MTU actuators were not strong enough to satisfy
216 the externally applied forces. As recommended by Hicks et al. [31], we ensured that these reserve
217 actuators provided no more than 5% of the total net moments at each degree of freedom to produce
218 valid simulations of muscle dynamics. The mechanical work generated from each MTU was
219 calculated by integrating the simulated power curves over the entire gait cycle.

220

221 **3. Results**

222 **(a) Experimental data**

223

224 LMMs found a significant ($p < 0.001$) effect of trial type (continuous walking and single trials) for
225 all spatiotemporal variables (Tables S2- 3), joint angles at heel-strike (Table S4) and toe-off (Table
226 S5) and all iEMG values (Tables S6-7). There were significant ($p < 0.05$) interaction effects between
227 substrate and trial type for most spatiotemporal variables (Tables S2- S3), joint angles (Tables S4-5)
228 and iEMG (Tables S6-7). However, for both trial types, substrate effects were similar; therefore,
229 when only individual trial data results are presented visually (Figs. 2-5), similar differences between
230 substrates also occurred on the continuous trials.

231

232 As substrate compliance increased, walking speed and stride width decreased and stride length,
233 cycle time, stance time, swing time and duty factor all increased significantly ($p < 0.001$) (Fig. 2,

234 Tables S2-3). The coefficient of variation (CV) was similar for speed but decreased by 8% and 12%
235 for stride length between floor and thin and thick foam, respectively. CV increased by 16% and
236 43% for stride width, 14% and 12% cycle time, 24% and 18% stance time and 28% and 24% swing
237 time between floor and thin and thick foam, respectively (Table S8). LMMs found a significant
238 ($p<0.001$) effect of speed for all spatiotemporal variables and significant ($p<0.001$) interaction
239 effects between speed and substrate for most spatiotemporal variables (Tables S9-10). LMMs found
240 a significant ($p<0.001$) effect of gender for stride length and stance time and cycle time, swing time
241 and duty factor ($p<0.05$). There were significant ($p<0.05$) interaction effects between gender, speed
242 and substrate for most spatiotemporal variables (Tables S9-10).

243

244 When averaged across each subject, E_{kin} and E_{tot} decreased over most of the stride as substrate
245 compliance increased (Fig. 3a). During most of the stride, E_{pot} increased on the foams, except
246 during early- to mid-stance (Fig. 3a). As substrate compliance increased, relative amplitude (RA)
247 increased by $\sim 4.6\%$ and $\sim 33.4\%$ (Fig. 3c) and congruity percentage (CO) decreased by $\sim 30\%$ and
248 $\sim 18\%$ between floor and thin/thick foams respectively (Fig. 3d). The recovery of the total energy
249 exchange (R) increased by $\sim 3.2\%$ between floor and thin foam but decreased by $\sim 3.7\%$ between
250 floor and thick foam (Fig. 3b). LMMs showed that the effect of substrate is significant for all
251 variables between most substrates ($p<0.05$) (Table S11). LMMs found a significant effect of speed
252 ($p<0.001$) and gender for all variables and some significant interaction effects between speed,
253 gender and substrate ($p<0.05$) (Table S11).

254

255 1D-SPM analyses of sagittal plane joint angles found significant differences between all substrates
256 at different stages of the stride (Fig. 4; Tables S12-14). During heel-strike, as substrate compliance
257 increased, there was a significant ($p<0.005$) increase in hip flexion (Fig. 4a), knee flexion (Fig. 4b)
258 and ankle plantarflexion (Fig. 4c) between all the substrates. LMMs at heel-strike showed that the
259 effect of substrate is significant ($p<0.001$) for hip angle on all substrates and between floor and

260 thick foam for knee angle (Table S15). Also, there was a significant effect of speed for hip angle
261 ($p<0.001$) and knee angle ($p<0.01$). At heel-strike, LMMs found no significant ($p>0.05$) effects for
262 ankle angle (Table S15). During early-stance, there was significantly less plantarflexion at the ankle
263 joint ($p<0.001$) on the foams and during late-stance, there was less dorsiflexion at the ankle joint
264 ($p<0.05$) on the foams (Fig. 4c). Throughout much of stance phase, hip and knee joint angles were
265 similar on all substrates. During toe-off, all joint angles were similar but the foot is in contact with
266 the foams for longer. LMMs at toe-off found a significant ($p<0.001$) effect for knee angle between
267 the floor and thick foam and between floor and thin foam ($p<0.05$) for ankle and knee angle (Table
268 S16). During swing, there were significant increases in plantarflexion at the ankle joint ($p<0.01$)
269 and in flexion at the knee ($p<0.001$) and hip joint ($p<0.001$) as substrate compliance increased (Fig.
270 4). There were also some significant ($p<0.05$) interaction effects between speed, gender and
271 substrate at both heel-strike and toe-off (Table S15-16).

272
273 Overall there was a small increase in muscle activity for all measured muscles as substrate
274 compliance increased (Fig. 5). However, nEMG for the TA (Fig. 5e) during heel-strike and toe-off
275 and for RF (Fig. 4b), VL (Fig. 5c), VM (Fig. 5d) during heel-strike were higher on the hard floor
276 than on the compliant surfaces. During mid-stance, on the hard floor, nEMG for the MG (Fig. 5f)
277 and LG (Fig. 5g) were also higher than on the foam substrates. This pattern is generally consistent
278 with iEMG values, which show increases for all muscles as substrate compliance increased, except
279 LG on the thin foam (Fig. 5i). LMMs for the iEMG values show the effect of substrate is significant
280 ($p<0.01$) for VM for all substrates, between floor and thin foam for BFL and LG ($p<0.05$) and
281 between floor and thick foam for TA ($p<0.01$) and MG ($p<0.001$) (Tables S17- 18). There was no
282 significant ($p>0.05$) effect of substrate for RF, VL and SOL. LMMs found a significant ($p<0.05$)
283 effect of speed for BFL, VL and VM, and gender for BFL, MG and SOL (Tables S17 - 18). There
284 were also some significant ($p<0.05$) interaction effects between speed, gender and substrate (Tables
285 S17-18).

286

287

288 **(b) Musculoskeletal modelling**

289 The CMC simulations produced valid representations of walking over the hard floor and the foam
290 surfaces. The outputs accurately replicated the energetics of the experimental subject, with
291 estimated CoT values of $2.77 \text{ Jkg}^{-1}\text{m}^{-1}$, $3.01 \text{ Jkg}^{-1}\text{m}^{-1}$ and $3.40 \text{ Jkg}^{-1}\text{m}^{-1}$ on the floor, thin and thick
292 foams respectively (compared to experimental values of $2.70 \text{ Jkg}^{-1}\text{m}^{-1}$, $3.11 \text{ Jkg}^{-1}\text{m}^{-1}$ and $3.99 \text{ Jkg}^{-1}\text{m}^{-1}$) and a good match between predicted activations and experimental EMG data in the majority
293 of muscles on all substrates (Fig. S5). Simulations predicted that positive and negative MTU power
294 and work increased with surface compliance in the muscles crossing the hip and knee joints (GMax,
295 BFL, RF, VL, VM; Fig. 6a-e), but decreased in the more distal muscles crossing the ankle (TA,
296 MG, LG, SOL; Fig. 6f-i). Specifically, the peak negative power produced by proximal muscles such
297 as GMax increased from -0.62 Wkg^{-1} on the floor to -1.63 Wkg^{-1} on the thick foam, while the peak
298 positive power produced by VL increased from 0.89 Wkg^{-1} to 2.51 Wkg^{-1} (Fig. 6d). This translated
299 to changes in positive and negative work from 0.03 Jkg^{-1} and -0.10 Jkg^{-1} to 0.26 Jkg^{-1} and -0.36 Jkg^{-1}
300 on the thick foam in GMax and from 0.20 Jkg^{-1} and -0.55 Jkg^{-1} to 0.61 Jkg^{-1} and -0.97 Jkg^{-1} in VL
301 (Fig. 6j). These patterns of power and work were different in the distal muscles such as LG, where
302 peak positive power decreased from 0.45 Wkg^{-1} on the floor to 0.33 Wkg^{-1} on the thick foam (Fig.
303 6h), which translated to decreases in positive and negative work from 0.04 Jkg^{-1} to -0.07 Jkg^{-1} to
304 0.03 Jkg^{-1} and -0.04 Jkg^{-1} (Fig. 6j).

306

307 These patterns of power and work in individual muscles were also seen at the functional muscle
308 group level (Fig. 6k). For instance, the hip and knee extensors produced more positive and negative
309 work on the thick foam (hip extensors = 0.57 Jkg^{-1} / -0.90 Jkg^{-1} ; knee extensors = 1.18 Jkg^{-1} / -2.01
310 Jkg^{-1}) relative to the hard floor (hip extensors = 0.12 Jkg^{-1} / -0.30 Jkg^{-1} ; hip extensors = 0.46 Jkg^{-1} / -

311 1.13 Jkg⁻¹), while this pattern was reversed in the ankle plantarflexors (thick foam = 0.11 Jkg⁻¹ / -
312 0.13 Jkg⁻¹; floor = 0.12 Jkg⁻¹ / -0.25 Jkg⁻¹).

313

314 **4. Discussion**

315 It has long been recognised that animals incur a higher energetic cost when moving on compliant
316 substrates like sand, snow and foam [6-8, 10, 13]. However, as noted by Davies and Mackinnon
317 [10], the methods and data used to elucidate the underlying mechanical causes of this increase have
318 varied considerably in the literature, while substrate properties are rarely quantified. By collecting a
319 comprehensive and relatively large experimental motion data set we were able to systematically
320 characterise changes in walking gait with substrate compliance, and, by combining data with
321 mechanical substrate testing, drive the first subject-specific computer simulations of human
322 locomotion on compliant substrates to estimate the altered internal kinetic demands on the
323 musculoskeletal system. These analyses lead us to reject a number of previous hypotheses related to
324 increased locomotor costs, and instead lead us to modify other previous mechanisms to propose a
325 more intricate explanatory model for increased energetic costs of walking on compliant terrains.

326

327 Our LMMs show that gender and walking speed have significant interaction effects in our statistical
328 models of spatiotemporal parameters and energy exchange variables (Tables S9-11). However, we
329 find no significant difference in CoT between males and females on any substrate (Fig. S6), which
330 is consistent with previous findings on hard substrates [32]. Furthermore, in a previous study we
331 found no statistically significant relationships between CoT and various morphological variables
332 that are likely to have gender biases such as lower limb length, body stature and maximum
333 isometric ankle plantarflexion torques [16]. Given these results, and more importantly that the
334 qualitative differences in kinematics between substrates are the same for males and females, we
335 conclude that gender does not influence this examination of the causative mechanisms underpinning

336 CoT increases on the foams generally and universally across the cohort. Walking speed has an
337 intrinsic mechanistic link with most gait parameters and as such it is not surprising that significant
338 interaction effects are recovered in the LMMs. Average walking speeds were 1.36m/s, 1.32m/s and
339 1.23m/s on the floor, thin and thick foams respectively, and these differences are recovered as
340 statistically significant. However, studies of changes in CoT with walking speeds on hard substrates
341 recover small increases in CoT as speed increases across the range observed here (e.g. [33]), in
342 contrast to our negative relationship between CoT and speed. Given this different polarity of change
343 in CoT, and the small magnitude of speed change, we suggest that as an isolated variable, speed is
344 not an important causative contributor to the observed increase in CoT across the substrates.

345

346 Walking is most efficient when the whole-body CoM moves in an inverted pendulum motion,
347 allowing for an optimal exchange of kinetic and potential energy between gait cycles [20]. It has
348 been proposed (HYP1) that disruptions to the inverted pendulum mechanics of walking contribute
349 to the observed increase in energetic costs on compliant substrates such as sand [6]. However, in
350 this study we observed little differences in the recovery of total energy exchange (R) with 57-61%
351 R found across all substrates (Fig. 3). Lejeune et al. [7] also found a relatively efficient pendular
352 mechanism when walking on sand with as much as 60% mechanical energy recovery despite sand
353 having low resilience. Our findings suggest that there is little to no disruption to the inverted
354 pendulum mechanics of walking on compliant substrates. We therefore reject HYP1.

355

356 The mechanical work needed to move CoM is directly related to the cost of walking, particularly at
357 step-to-step transitions [34, 35]. Stance phase is important as it requires active braking with the
358 absorption of external power, followed by active propulsion to allow the CoM to be directed
359 towards the opposite side. Pontzer et al. [36] found a strong correlation between CoT and estimated
360 volume of muscle activated per metre travelled. Based on previous work, we hypothesised (HYP2a)

361 that increased muscle activation either throughout the limb [3] or (HYP2b) within specific muscle
362 groups [14] was responsible for increased energetic costs on compliant terrains. Overall we saw
363 increased activation in all measured muscles (Fig. 5), partially supporting HYP2a. Bates et al. [14]
364 previously suggested that walking on compliant substrates will increase energetic costs as greater
365 muscle-tendon forces are required by the ankle extensors to generate the propulsion needed from
366 mid-stance to reaccelerate into the swing phase. In partial support of this, we found slightly
367 increased ankle extensor values during terminal stance- or push-off on the foams. However, our
368 computer simulations suggest there is no increase in the mechanical work done by the TA (Fig. 6f),
369 MG (Fig. 6g), LG (Fig. 6h) and SOL (Fig. 6i) during mid-stance to push-off on these compliant
370 substrates compared to the hard floor. These findings (and others; see below) indicate, that while
371 muscle activations do increase on compliant terrains, these increases do not uniformly or
372 simplistically translate into increased locomotor costs, suggesting HYP2 is too simplistic as a
373 standalone explanation.

374

375 In similar vein, we find partial support for (HYP3) increased MTU work and decreased efficiency,
376 but our results (Fig. 6) emphasise a much more complex pattern across MTUs on compliant
377 substrates [7, 8]. While our simulations predicted that positive and negative MTU power and work
378 increased with substrate compliance in muscles crossing the hip and knee joints (GMax, BFL, RF,
379 VL, VM; Fig. 6a-e), a decrease (contra HYP3) was predicted in the more distal muscles crossing
380 the ankle (Fig. 6). These patterns of muscle activation (Fig. 5) and power production (Fig. 6) are
381 related to the significant kinematic differences on the three substrates, most notably at heel-strike
382 and during swing (Figs. 2-4). When the joints are more flexed and less aligned with the resultant
383 ground reaction force, a greater volume of active muscle is required [36]. In particular, increased
384 hip and knee flexion is clearly mechanistically related to greater mechanical work done by the
385 muscles crossing the knee and hip joints (Gmax, BFL, RF, VL, VM) (Fig. 6). Previous studies have
386 suggested that walking on uneven or irregular terrain [1, 3, 4] also incurs increased mechanical

387 work at the knee and hip due to greater knee and hip flexion, and thus the patterns of muscle
388 activation and force production recovered here may apply to other terrain types with elevated
389 energetic costs.

390

391 The nature and magnitude of changes in ankle joint kinematics are consistent with the little or no
392 increase in mechanical work seen in distal limb muscles in our simulations (Fig. 6). Here, a larger
393 total joint excursion (i.e. the range of motion through both greater maximum dorsiflexion and
394 plantarflexion angles) is observed on the hard floor during stance rather than foams, where ankle
395 angle remains relatively constant during midstance (Fig. 4a) compared to the continuous
396 dorsiflexion observed on the hard floor. nEMG data (Fig. 5a) suggests greater activation of LG, MG
397 and to a lesser extent SOL during midstance on the hard floor, with active dorsiflexion of the ankle
398 suggesting that activation of these muscles is eccentric versus near-isometric on the foams (Fig. 4a).
399 As a result, these muscles are predicted to incur greater negative mechanical power and work
400 during stance on the hard floor compared to the foams (Fig. 6). Therefore we propose that previous
401 hypotheses that changes in muscle kinetics and energetics (HYPs 2 and 3; [3, 7]) should be refined,
402 and that increased mechanical work at the knee and hip due to greater flexion and overall joint
403 excursion, is primarily responsible for increased energetics costs on compliant substrates, with
404 negligible contribution from distal muscles.

405

406 These changes to joint kinematic and associated muscle kinetics are mechanistically related to the
407 changes observed in spatiotemporal gait parameters (Fig. 2). We found that more compliant
408 substrates resulted in significant increases in stride length, cycle time, stance time, swing time and
409 duty factor, but decreases in speed and stride width (Fig. 2). Cotes and Meade [37] found an
410 increase in step length resulting in greater vertical displacements of the CoM. Previous simulation
411 [38] and experimental [34] studies also concluded that larger steps increased energetic costs due to

412 CoM redirection. Slower stride frequencies, rather than reduced stride length, account for the
413 observed slower speeds. However, previous studies on slippery surfaces have observed slower
414 walking speeds with shorter stride lengths and flatter foot-floor angles at heel-strike, possibly to
415 keep the CoM centred over the supporting limb to improve stability [39, 40]. The increase in cycle
416 time, stance time, swing time and duty factor are partly due to the reduction in speed, however, the
417 increase in duty factor on compliant substrates suggests there is a proportionally longer stance time.
418 As peak ground reaction forces will be lower on compliant substrates, an increase in stance time
419 ensures there is enough time to exert force on the ground to redirect the CoM. This reduction in
420 efficiency for the redirection of the CoM would produce an increase in mechanical work and thus,
421 consume more metabolic energy. Similar mechanisms are observed in smaller animals [41], in
422 young children [42] and adults walking on uneven terrain [3, 4] who adopt a more crouched gait,
423 coupled with an increase in stance time, to ameliorate the power costs. These changes are ultimately
424 inter-linked with the postural or kinematic changes (Fig. 4), and their muscular mechanisms (Fig. 6)
425 observed here (see below).

426

427 It was also hypothesised that (HYP4) correcting greater instabilities indicated by increased
428 variability in gait [13] increase energetic costs. While, there was no change in CV for speed and a
429 decrease in CV for stride length, we found large increases in CV for stride width, cycle time, stance
430 time and swing time on the compliant foams compared to the hard floor (Table S8). However, while
431 previous studies that have correlated increased step-to-step variability with increased CoT, they
432 have noted that even relatively high levels of variability yield modest increases in metabolic costs
433 [43, 44]. For example, O'connor [43] found that a 65% increase in step width variability was
434 correlated with a 5.9% increase in energetic costs. Here we find lesser increases in CV for stride
435 width on the foam but greater increases in CoT. Therefore, while we find support for HYP4, we
436 infer that changes in hip and knee joint kinematics and kinetics represent the major contributor to
437 increased CoT on compliant substrates.

438

439 Here, we chose foams as the focus substrate and through material testing of mechanical properties
440 we were able to simulate locomotion on compliant terrain using a highly detailed musculoskeletal
441 model for the first time. This leads us to present an explanatory model of CoT increase in which
442 elevated activity and mechanical work by muscles crossing the hip and knee are required to support
443 the changes in joint (greater excursion and maximum flexion) and spatiotemporal kinematics
444 (longer stride lengths, stride times and stance times, and duty factors) on compliant substrates.
445 Other compliant substrates, such as sand (and indeed even other types of foams) likely exhibit
446 different mechanical properties to our foams, in addition to other responses (e.g. foot slippage [6])
447 and therefore the extent to which our explanatory factors apply universally to compliant terrains
448 remains to be tested. Huang et al. [45] found that reduced ankle push-off, and greater collisional
449 losses, resulted in greater positive work throughout the gait cycle, as well as compensations at the
450 other joints, particularly at the knee joint. Furthermore, they found increased mechanical work at
451 the lower limb joints resulted in greater energy expenditure, in support of our proposed model [45].
452 We hypothesise that the modified joint kinematics and spatiotemporal kinematics, and associated
453 increase in muscle work at the hip and knee, are likely to occur (albeit to varying degrees) on most
454 compliant substrates in healthy adult subjects, and therefore the model of CoT increase we present
455 here will be widely applicable for similar human populations, and potentially mammals more
456 widely where relatively upright limb postures are utilised. It would also be interesting for future
457 work to explore changes in musculoskeletal mechanics on compliant substrates in animals that
458 utilise more crouched postures. For example, birds typically use considerably less hip motion than
459 humans and power the stride predominantly from the knee and ankle joints [46]. It is therefore
460 possible that greater responses to changes in substrate compliance may be observed in distal, rather
461 than proximal, joints in birds and other animals with crouched postures.

462

463 **5. Conclusion**

464 Our analyses lead us to reject a number of previous hypotheses related to increased locomotor costs,
465 such as disruptions to the inverted pendulum mechanics and increased mechanical work at distal
466 limb muscles. Instead we find that the mechanistic causes of increased energetic costs on compliant
467 substrates lie predominantly in the proximal limb and are more complex than captured by any single
468 previous hypothesis. Specifically, elevated activity and greater mechanical work by muscles
469 crossing hip and knee are required to support the changes in joint (greater excursion and maximum
470 flexion) and spatiotemporal kinematics (longer stride lengths, stride times, stance times, duty
471 factors and increased variability) on our compliant substrates. The validation of a computer
472 simulation of locomotion on compliant substrates herein demonstrates the potential of this approach
473 to explore morphological and mechanical adaptations to different substrates in other animal groups.

474

475

476 **Ethics**

477 All participants signed informed consent before participating in the study in accordance with ethical
478 approval from the University of Liverpool's Central University Research Ethics Committee for
479 Physical Interventions (#3757).

480

481 **Data accessibility**

482 Experimental data and code for analysis and figure generation can be found at the following link:

483 <https://doi.org/10.5061/dryad.6hdr7sr31>

484 The data are provided in electronic supplementary material [47].

485

486 **Author Contributions**

487 B.F.G.: data curation, formal analysis, investigation, methodology, writing- original draft, writing-
488 review and editing; J.C.: data curation, formal analysis, investigation, methodology, writing-
489 original draft, writing- review and editing; B.G.: data curation, formal analysis, investigation,
490 methodology, resources, writing- original draft; J.G.: formal analysis, methodology, writing- review
491 and editing; K.D.: conceptualisation, funding acquisition, methodology, resources, supervision,
492 writing- review and editing; P.L.F.: conceptualisation, funding acquisition, methodology,
493 supervision, writing- review and editing; K.T.B.: conceptualisation, data curation, funding
494 acquisition, investigation, methodology, project administration, resources, supervision, writing-
495 original draft, writing- review and editing.

496

497 All authors gave final approval for publication and agreed to be held accountable for the work
498 performed therein.

499

500 **Funding**

501 This study was funded by grants from the Leverhulme Trust (RPG-2017-296) and by the Medical
502 Research Council (MRC) and Versus Arthritis as part of the Medical Research Council Versus
503 Arthritis Centre for Integrated Research into Musculoskeletal Ageing (CIMA) [MR/P020941/1].
504 The MRC Versus Arthritis Centre for Integrated Research into Musculoskeletal Ageing is a
505 collaboration between the Universities of Liverpool, Sheffield and Newcastle.

506

507 **References**

- 508 1 Gates, D. H., Wilken, J. M., Scott, S. J., Sinitski, E. H., Dingwell, J. B. 2012 Kinematic strategies
509 for walking across a destabilizing rock surface. *Gait & Posture*. **35**, 36-42.
510 (<https://doi.org/10.1016/j.gaitpost.2011.08.001>)
511 2 Wade, C., Redfern, M. S., Andres, R. O., Breloff, S. P. 2010 Joint kinetics and muscle activity
512 while walking on ballast. *Human Factors*. **52**, 560-573. (10.1177/0018720810381996)

- 513 3 Voloshina, A. S., Kuo, A. D., Daley, M. A., Ferris, D. P. 2013 Biomechanics and energetics of
514 walking on uneven terrain. *Journal of Experimental Biology*. **216**, 3963-3970.
515 (10.1242/jeb.081711)
- 516 4 Holowka, N. B., Kraft, T. S., Wallace, I. J., Gurven, M., Venkataraman, V. V. 2022 Forest
517 terrains influence walking kinematics among indigenous Tsimane of the Bolivian Amazon.
518 *Evolutionary Human Sciences*. **4**, e19. (10.1017/ehs.2022.13)
- 519 5 Soule, R. G., Goldman, R. F. 1972 Terrain coefficients for energy cost prediction. *Journal of*
520 *Applied Physiology*. **32**, 706-708. (10.1152/jappl.1972.32.5.706)
- 521 6 Zamparo, P., Perini, R., Orizio, C., Sacher, M., Ferretti, G. 1992 The energy cost of walking or
522 running on sand. *European Journal of Applied Physiology and Occupational Physiology*. **65**, 183-
523 187. (10.1007/BF00705078)
- 524 7 Lejeune, T. M., Willems, P. A., Heglund, N. C. 1998 Mechanics and energetics of human
525 locomotion on sand. *Journal of Experimental Biology*. **201**, 2071-2080. (10.1242/jeb.201.13.2071)
- 526 8 Pinnington, H. C., Dawson, B. 2001 The energy cost of running on grass compared to soft dry
527 beach sand. *Journal of Science and Medicine in Sport*. **4**, 416-430. ([https://doi.org/10.1016/S1440-
528 2440\(01\)80051-7](https://doi.org/10.1016/S1440-2440(01)80051-7))
- 529 9 Kerdok, A. E., Biewener, A. A., McMahon, T. A., Weyand, P. G., Herr, H. M. 2002 Energetics
530 and mechanics of human running on surfaces of different stiffnesses. *Journal of Applied*
531 *Physiology*. **92**, 469-478. (10.1152/jappphysiol.01164.2000)
- 532 10 Davies, S. E. H., Mackinnon, S. N. 2006 The energetics of walking on sand and grass at various
533 speeds. *Ergonomics*. **49**, 651-660. (10.1080/00140130600558023)
- 534 11 Stearne, S. M., McDonald, K. A., Alderson, J. A., North, I., Oxnard, C. E., Rubenson, J. 2016
535 The foot's arch and the energetics of human locomotion. *Scientific reports*. **6**, 19403.
536 (10.1038/srep19403)
- 537 12 Ray, S. F., Takahashi, K. Z. 2020 Gearing up the human ankle-foot system to reduce energy cost
538 of fast walking. *Scientific reports*. **10**, 8793. (10.1038/s41598-020-65626-5)
- 539 13 Pandolf, K. B., Haisman, M. F., Goldman, R. F. 1976 Metabolic energy expenditure and terrain
540 coefficients for walking on snow. *Ergonomics*. **19**, 683-690. (10.1080/00140137608931583)
- 541 14 Bates, K. T., Savage, R., Pataky, T. C., Morse, S. A., Webster, E., Falkingham, P. L., Ren, L.,
542 Qian, Z., Collins, D., Bennett, M. R., *et al.* 2013 Does footprint depth correlate with foot motion
543 and pressure? *J R Soc Interface*. **10**, 20130009. (10.1098/rsif.2013.0009)
- 544 15 Charles, J. P., Grant, B., D'Août, K., Bates, K. T. 2020 Subject-specific muscle properties from
545 diffusion tensor imaging significantly improve the accuracy of musculoskeletal models. *Journal of*
546 *anatomy*. **237**, 941-959.
- 547 16 Charles, J. P., Grant, B., D'Août, K., Bates, K. T. 2021 Foot anatomy, walking energetics, and
548 the evolution of human bipedalism. *Journal of human evolution*. **156**, 103014.
549 (<https://doi.org/10.1016/j.jhevol.2021.103014>)
- 550 17 Hanavan Jr, E. P. 1964 A mathematical model of the human body: Air Force Aerospace Medical
551 Research Lab Wright-patterson AFB OH.
- 552 18 Zeni Jr, J., Richards, J., Higginson, J. 2008 Two simple methods for determining gait events
553 during treadmill and overground walking using kinematic data. *Gait & posture*. **27**, 710-714.
- 554 19 Hermens, H. J., Freriks, B., Disselhorst-Klug, C., Rau, G. 2000 Development of
555 recommendations for SEMG sensors and sensor placement procedures. *Journal of*
556 *Electromyography and Kinesiology*. **10**, 361-374. ([https://doi.org/10.1016/S1050-6411\(00\)00027-
557 4](https://doi.org/10.1016/S1050-6411(00)00027-4))
- 558 20 Cavagna, G. A., Thys, H., Zamboni, A. 1976 The sources of external work in level walking and
559 running. *J Physiol*. **262**, 639-657. (10.1113/jphysiol.1976.sp011613)
- 560 21 Pataky, T. C., Robinson, M. A., Vanrenterghem, J. 2013 Vector field statistical analysis of
561 kinematic and force trajectories. *Journal of biomechanics*. **46**, 2394-2401.
562 (<https://doi.org/10.1016/j.jbiomech.2013.07.031>)

563 22 Fukuchi, C. A., Fukuchi, R. K., Duarte, M. 2019 Effects of walking speed on gait biomechanics
564 in healthy participants: a systematic review and meta-analysis. *Systematic Reviews*. **8**, 153.
565 (10.1186/s13643-019-1063-z)

566 23 Chumanov, E. S., Wall-Scheffler, C., Heiderscheit, B. C. 2008 Gender differences in walking
567 and running on level and inclined surfaces. *Clinical Biomechanics*. **23**, 1260-1268.
568 (<https://doi.org/10.1016/j.clinbiomech.2008.07.011>)

569 24 Team, R. C. R: A language and environment for statistical computing.

570 25 Bates, D., Mächler, M., Bolker, B., Walker, S. 2014 Fitting linear mixed-effects models using
571 lme4. *arXiv preprint arXiv:1406.5823*.

572 26 Kunzetsova, A., Brockhoff, P., Christensen, R. 2017 lmerTest package: Tests in linear mixed
573 effect models. *J Stat Softw*. **82**, 1-26.

574 27 ASTM, D. 2001 3574—Standard test methods for flexible cellular materials—slab. *Bonded, and*
575 *Molded Urethane Foams*. **164**,

576 28 Seth, A., Hicks, J. L., Uchida, T. K., Habib, A., Dembia, C. L., Dunne, J. J., Ong, C. F., DeMers,
577 M. S., Rajagopal, A., Millard, M., *et al.* 2018 OpenSim: Simulating musculoskeletal dynamics and
578 neuromuscular control to study human and animal movement. *PLOS Computational Biology*. **14**,
579 e1006223. (10.1371/journal.pcbi.1006223)

580 29 Charles, J. P., Grant, B., D'Août, K., Bates, K. T. 2020 Subject-specific muscle properties from
581 diffusion tensor imaging significantly improve the accuracy of musculoskeletal models. *Journal of*
582 *Anatomy*. **237**, 941-959. (<https://doi.org/10.1111/joa.13261>)

583 30 Sherman, M. A., Seth, A., Delp, S. L. 2011 Simbody: multibody dynamics for biomedical
584 research. *Procedia IUTAM*. **2**, 241-261. (<https://doi.org/10.1016/j.piutam.2011.04.023>)

585 31 Hicks, J. L., Uchida, T. K., Seth, A., Rajagopal, A., Delp, S. L. 2015 Is my model good enough?
586 Best practices for verification and validation of musculoskeletal models and simulations of
587 movement. *Journal of Biomechanical Engineering*. **137**, (10.1115/1.4029304)

588 32 Weyand, P. G., Smith, B. R., Puyau, M. R., Butte, N. F. 2010 The mass-specific energy cost of
589 human walking is set by stature. *Journal of Experimental Biology*. **213**, 3972-3979.
590 (10.1242/jeb.048199)

591 33 Abe, D., Yanagawa, K., Niihata, S. 2004 Effects of load carriage, load position, and walking
592 speed on energy cost of walking. *Applied Ergonomics*. **35**, 329-335.
593 (<https://doi.org/10.1016/j.apergo.2004.03.008>)

594 34 Donelan, J. M., Kram, R., Kuo, A. D. 2002 Mechanical work for step-to-step transitions is a
595 major determinant of the metabolic cost of human walking. *Journal of Experimental Biology*. **205**,
596 3717-3727. (10.1242/jeb.205.23.3717)

597 35 Kuo, A. D., Donelan, J. M., Ruina, A. 2005 Energetic Consequences of Walking Like an
598 Inverted Pendulum: Step-to-Step Transitions. *Exercise and Sport Sciences Reviews*. **33**, 88-97.

599 36 Pontzer, H., Raichlen, D. A., Sockol, M. D. 2009 The metabolic cost of walking in humans,
600 chimpanzees, and early hominins. *Journal of human evolution*. **56**, 43-54.
601 (<https://doi.org/10.1016/j.jhevol.2008.09.001>)

602 37 Cotes, J., Meade, F. 1960 The energy expenditure and mechanical energy demand in walking.
603 *Ergonomics*. **3**, 97-119.

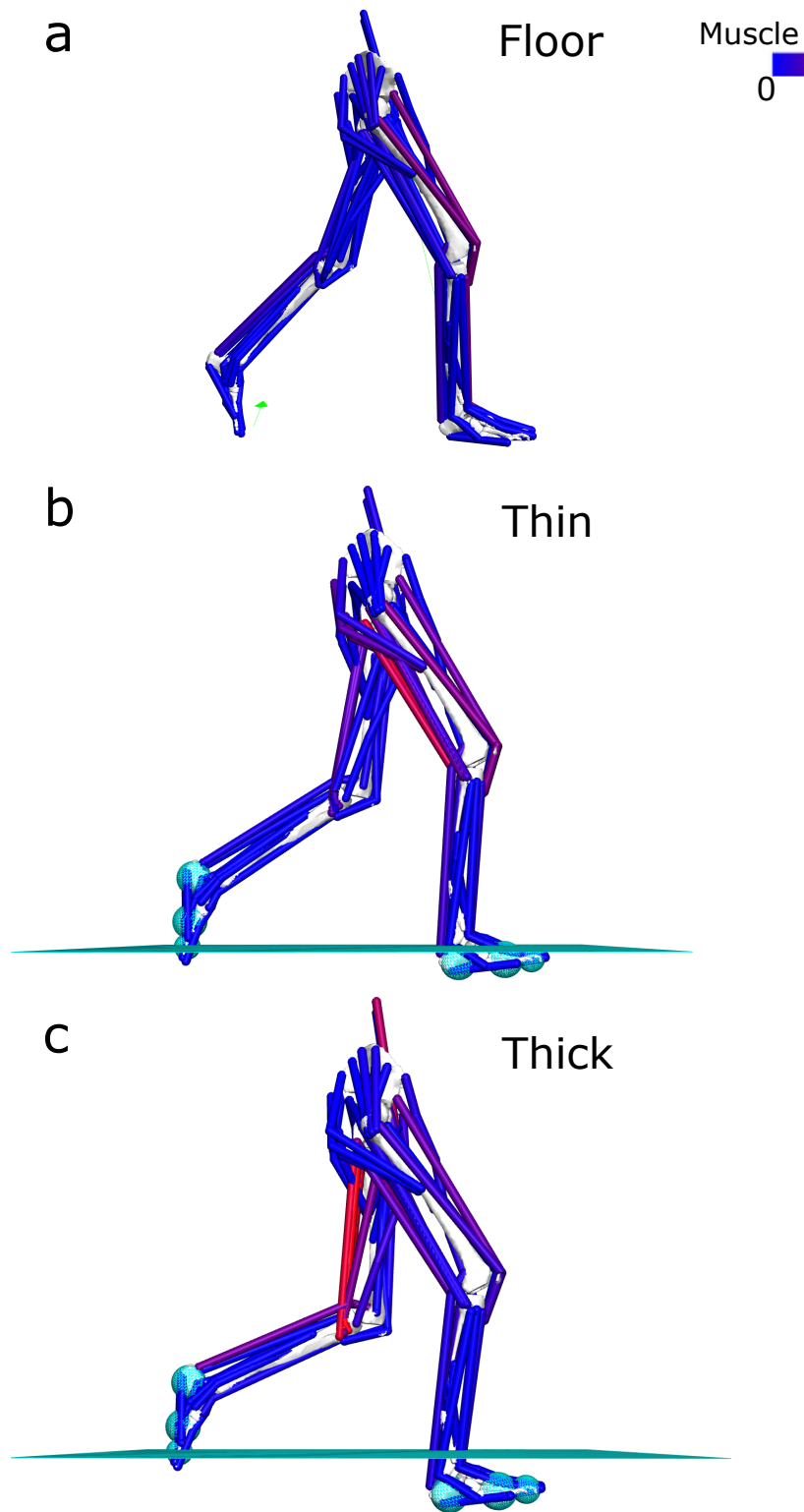
604 38 Faraji, S., Wu, A. R., Ijspeert, A. J. 2018 A simple model of mechanical effects to estimate
605 metabolic cost of human walking. *Scientific reports*. **8**, 10998. (10.1038/s41598-018-29429-z)

606 39 Cappellini, G., Ivanenko, Y. P., Dominici, N., Richard, E., Lacquaniti, F. 2010 Motor Patterns
607 During Walking on a Slippery Walkway. *Journal of Neurophysiology*. **103**, 746-760.
608 (10.1152/jn.00499.2009)

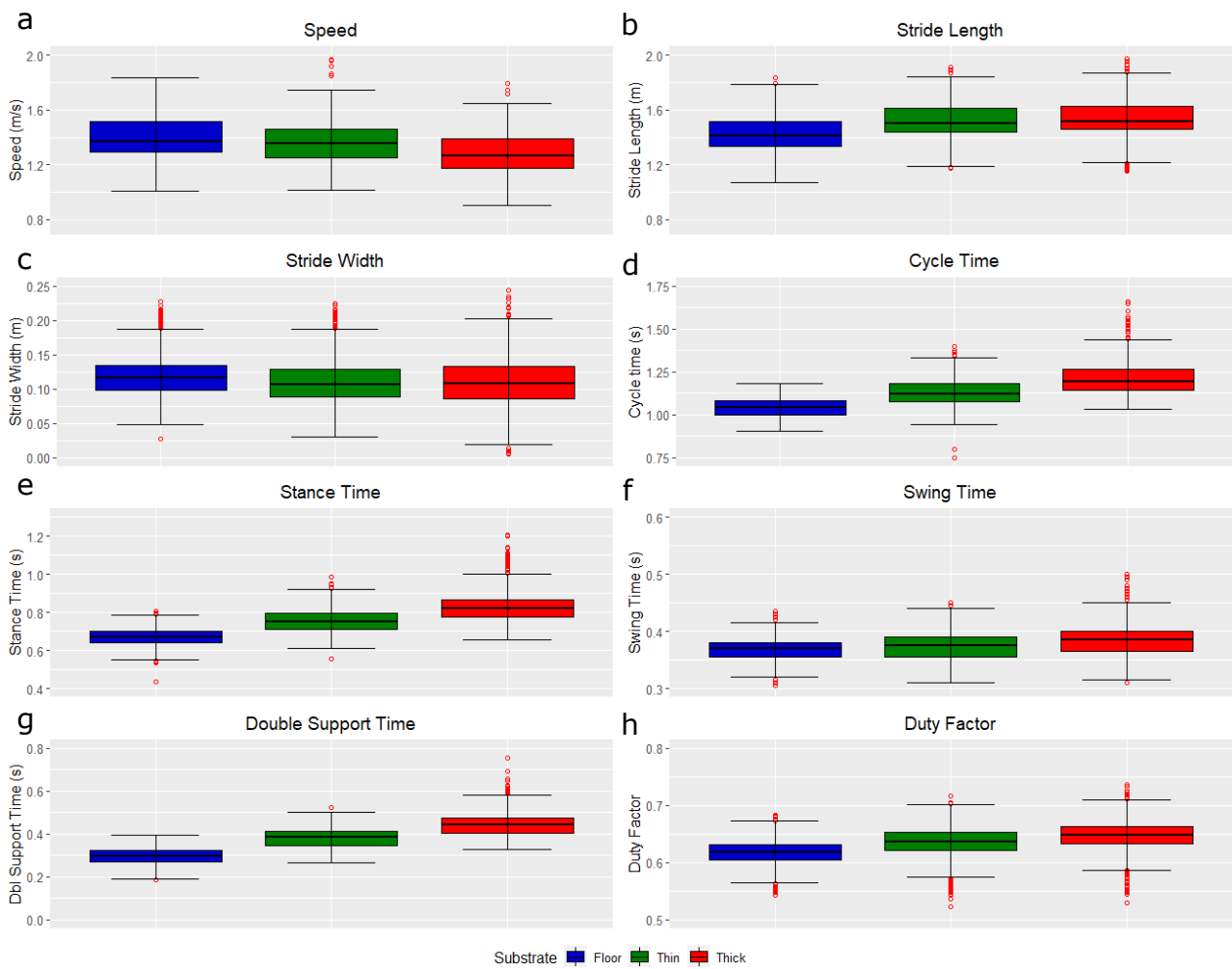
609 40 Cham, R., Redfern, M. S. 2002 Changes in gait when anticipating slippery floors. *Gait Posture*.
610 **15**, 159-171. (10.1016/s0966-6362(01)00150-3)

611 41 Usherwood, J. R. 2013 Constraints on muscle performance provide a novel explanation for the
612 scaling of posture in terrestrial animals. *Biology Letters*. **9**, 20130414.
613 (doi:10.1098/rsbl.2013.0414)

614 42 Hubel, T. Y., Usherwood, J. R. 2015 Children and adults minimise activated muscle volume by
615 selecting gait parameters that balance gross mechanical power and work demands. *Journal of*
616 *Experimental Biology*. **218**, 2830-2839. (10.1242/jeb.122135)
617 43 O'Connor, S. M., Xu, H. Z., Kuo, A. D. 2012 Energetic cost of walking with increased step
618 variability. *Gait & Posture*. **36**, 102-107. (<https://doi.org/10.1016/j.gaitpost.2012.01.014>)
619 44 Donelan, J. M., Shipman, D. W., Kram, R., Kuo, A. D. 2004 Mechanical and metabolic
620 requirements for active lateral stabilization in human walking. *Journal of biomechanics*. **37**, 827-
621 835. (<https://doi.org/10.1016/j.jbiomech.2003.06.002>)
622 45 Huang, T.-w. P., Shorter, K. A., Adamczyk, P. G., Kuo, A. D. 2015 Mechanical and energetic
623 consequences of reduced ankle plantar-flexion in human walking. *Journal of Experimental Biology*.
624 **218**, 3541-3550. (10.1242/jeb.113910)
625 46 Gatesy, S. M., Biewener, A. A. 1991 Bipedal locomotion: effects of speed, size and limb posture
626 in birds and humans. *Journal of Zoology*. **224**, 127-147. ([https://doi.org/10.1111/j.1469-](https://doi.org/10.1111/j.1469-7998.1991.tb04794.x)
627 [7998.1991.tb04794.x](https://doi.org/10.1111/j.1469-7998.1991.tb04794.x))
628 47 Grant, Barbara (2022), Why does the metabolic cost of walking increase on compliant
629 substrates?, Dryad, Dataset, <https://doi.org/10.5061/dryad.6hdr7sr31>
630

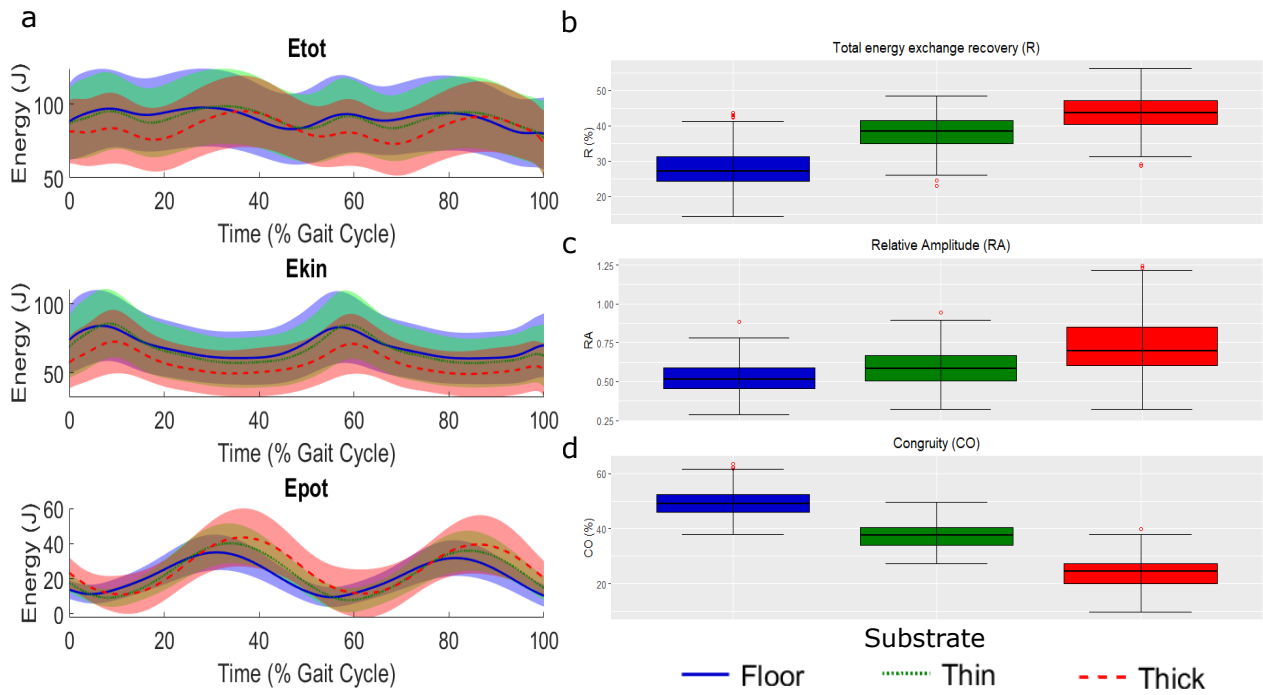


632
633 **Figure 1.** Lateral views of the subject-specific models and simulations of walking on the (a) floor,
634 (b) thin foam and (c) thick foam, with predicted muscle activations shown. The cyan planes in (a)
635 and (b) represent the top surface of the foams.
636
637
638



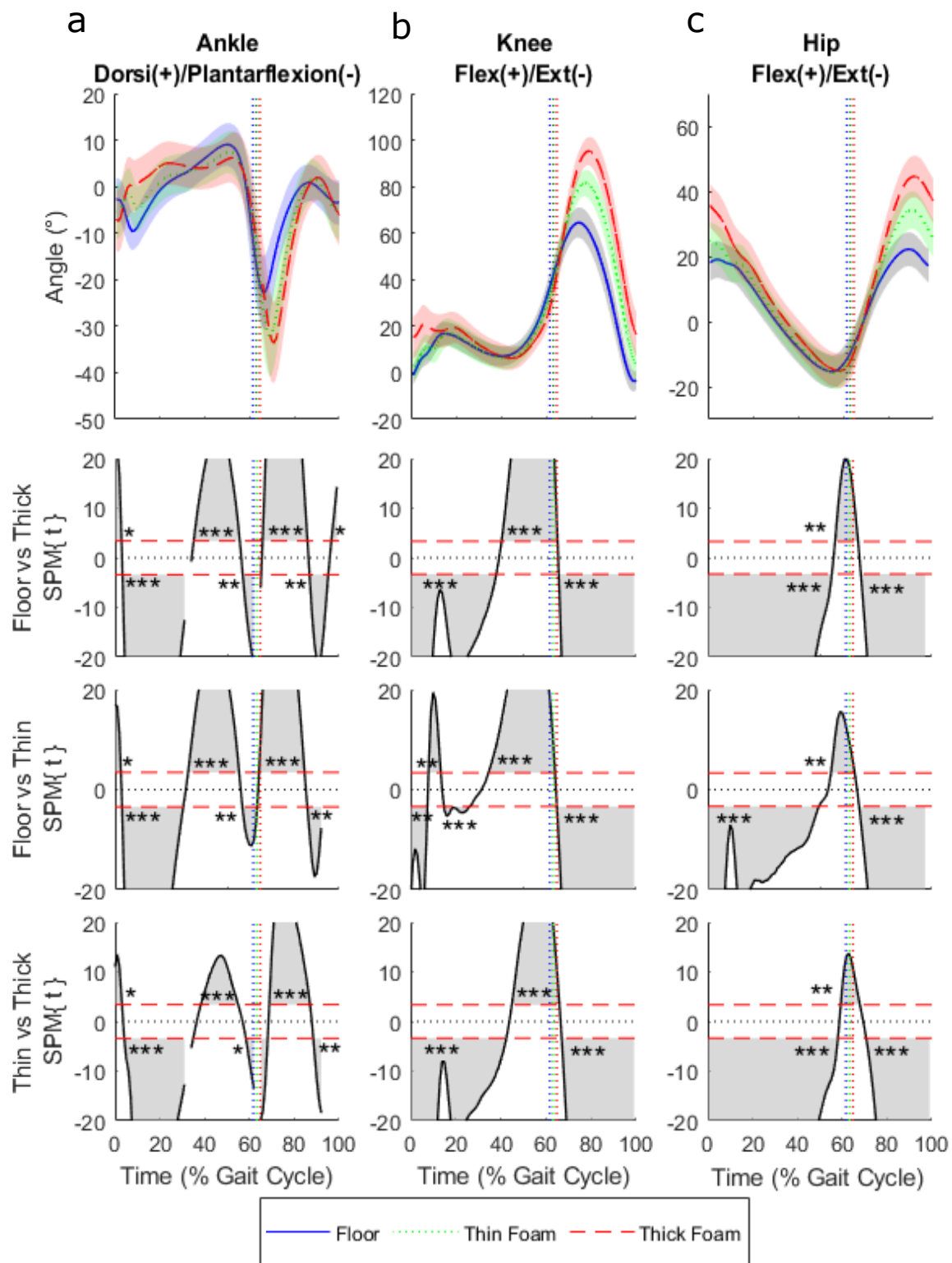
639
 640
 641
 642
 643
 644
 645
 646
 647

Figure 2. The distribution of spatio-temporal parameters for all participants combined (n=30) while walking on the three different substrates: floor (blue), thin foam (green) and thick foam (red). (a) speed, (b) stride length, (c) stride width, (d) cycle time, (e) stance time, (f) swing time, (g) double support time and (h) duty factor. Data includes all strides for individual trials (n = 5023). Red circles denote an individual stride from any subject that represents a statistical outlier.



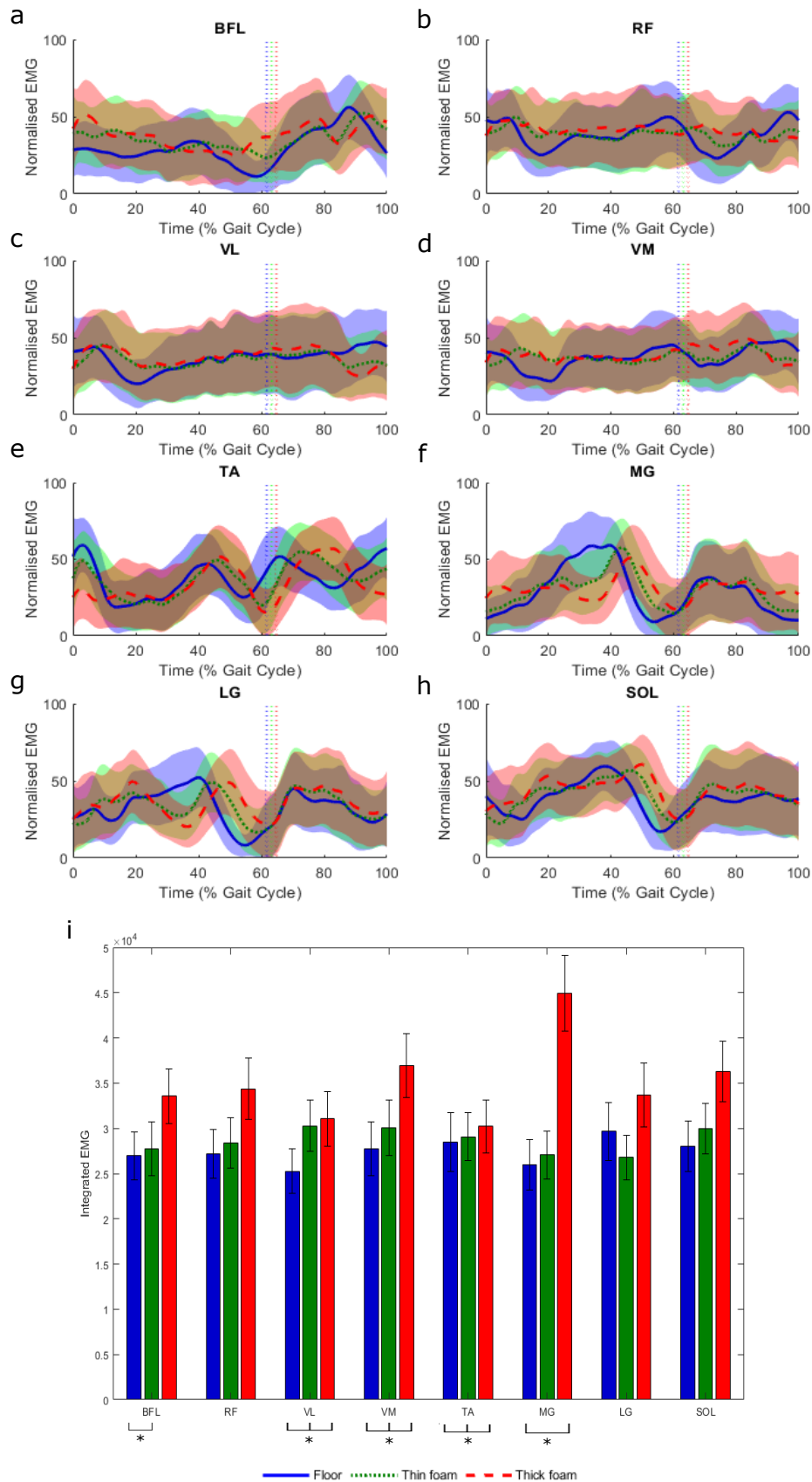
648
 649 **Figure 3.** (a) Mass-normalised total (E_{tot}) mechanical energy (top), kinetic (E_{kin}) energy (middle)
 650 and the gravitational potential (E_{pot}) energy of the COM (bottom) and normalised to walking stride
 651 for all participants combined ($n=30$) while walking on the three different substrates (mean \pm s.d)
 652 ($n=2935$). The distribution of pendulum-like determining variables: (b) The recovery of total energy
 653 exchange as a percentage (R), (c) Relative Amplitude (RA), and (d) Congruity percentage (CO) for
 654 all participants combined ($n=30$) while walking on the three different substrates. Floor (blue), thin
 655 foam (green) and thick foam (red). Red circles denote an individual stride from any subject that
 656 represent statistical outlier.
 657

658



659
 660 **Figure 4.** (a) Ankle, (b) knee and (c) hip joint angles in the sagittal plane for all participants
 661 combined (n=30) while walking on the three different substrates: floor (blue), thin foam (green) and
 662 thick foam (red). The vertical dotted lines indicate toe-off. 1D-SPM (utilising paired t-tests with
 663 Bonferroni corrections) indicate regions of statistically significant differences between walking
 664 conditions, when 1D-SPM lines exceed the critical threshold values denoted by the horizontal red
 665 dotted lines. Shaded regions (within the SPM graphs) correspond to the period within the gait cycle

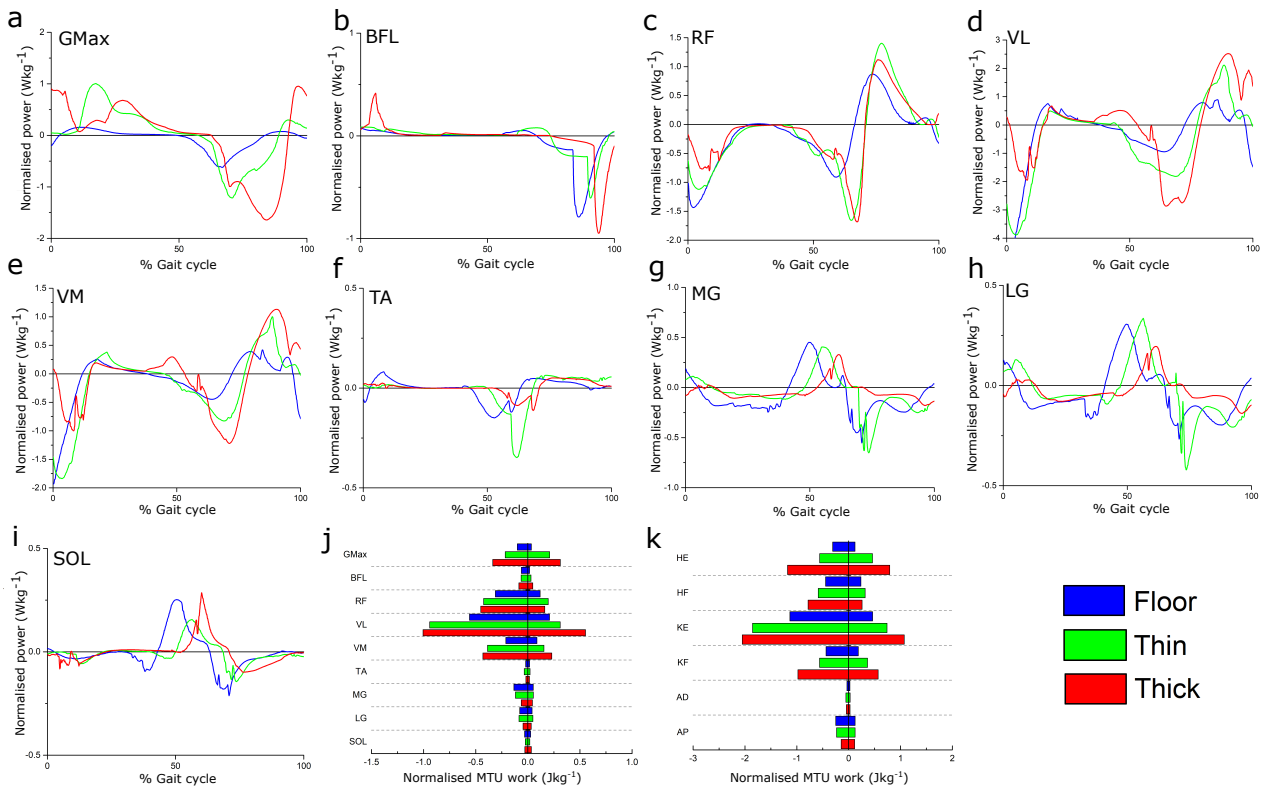
666 where walking conditions are statistically significantly different from one another. “*, **, ***”
667 represent p-values of less than 0.05, 0.01 and 0.001 respectively.
668
669
670



671
672
673
674
675

Figure 5. nEMG values for 8 left lower extremity muscles for participants combined (n=24) while walking on the three different substrates: floor (blue), thin foam (green) and thick foam (red) (a) biceps femoris (BFL), (b) rectus femoris (RF), (c) vastus lateralis (VL), (d) vastus medialis (VM), (e) tibialis anterior (TA), (f) lateral gastrocnemius (LG), (g) medial gastrocnemius (MG) and (h)

676 soleus (SOL) (mean \pm s.d.). The vertical dotted lines indicate toe-off. **(i)** iEMG values (mean \pm
677 s.d.). Asterisks indicates significant differences between substrates ($p < 0.05$).



678

679 **Figure 6.** Normalised power (Wkg^{-1} ; a-i) and mechanical work (Jkg^{-1} ; j) outputs from select lower
 680 limb musculotendon units (MTU), as well as functional group totals (k), as predicted by subject-
 681 specific simulations of walking on the floor as well as the thin and thick foam substrates. Power and
 682 work both tended to increase in the more proximal MTUs on the more compliant substrates relative
 683 to the floor, however this trend was reversed in the more distal MTUs. GMax- gluteus maximus,
 684 BFL- biceps femoris (long head), RF- rectus femoris, VL- vastus lateralis, VM- vastus medialis,
 685 TA- tibialis anterior, MG- medial gastrocnemius, LG- lateral gastrocnemius, SOL- soleus, HE- Hip
 686 extensors (GMax, BFL, semimembranosus, semitendinosus), HF- Hip flexors (iliacus, psaos, RF),
 687 KE- Knee extensors (RF, VL, VM, vastus intermedius), KF- Knee flexors (BFL, biceps femoris
 688 short head, semimembranosus, semitendinosus), AD- Ankle dorsiflexors (TA, extensor digitorum
 689 longus, extensor hallucis longus), AP- Ankle plantarflexors (MG, LG, SOL, flexor digitorum
 690 longus, flexor hallucis longus, tibialis posterior).

691